Hindawi
International Journal of Rotating Machinery
Volume 2018, Article ID 5051794, 7 pages
https://doi.org/10.1155/2018/5051794

Research Article

Influence of Spiral Angle on the Performance of Spiral Oil Wedge Sleeve Bearing

Li-li Wang, Qing-liang Zeng, and Xin Zhang

College of Mechanical and Electronic Engineering, Shandong University of Science and Technology, Qingdao 266590, China

Correspondence should be addressed to Qing-liang Zeng; 1600793307@qq.com

Received 27 December 2017; Revised 19 April 2018; Accepted 26 April 2018; Published 5 June 2018

Academic Editor: Farid Bakir

Spiral angel is an important structure parameter of spiral oil wedge sleeve bearing, which produces greater impact on bearing performance. Based on JFO boundary condition, the generalized Reynolds equations considering four slip conditions are established. Using the concept of partial derivatives, stiffness and damping coefficients of sleeve bearing are calculated. The results show that carrying capacity and friction drag of oil film decrease, temperature rise decreases first and then increases, and end leakage rate, stiffness, and damping coefficients generally increase first and then decrease with the increase of spiral angle. The carrying capacity, friction drag, temperature rise, stiffness, and damping coefficients are smaller and the end leakage rate is higher considering wall slip and JFO condition compared with reckoning with no slip and Reynolds boundary condition.

1. Introduction

Sleeve bearings are widely used in rotating machinery, and oil film force is an important factor that affects the stability of rotor system. At the current state of research on improving the stability performance of hydrodynamic bearings, there are several in-depth studies taking into account the journal misalignment, the bearing surface roughness, the cavitation phenomenon, and the impact of the texturing. And the effect of structural parameters on bearing stability can not be ignored, especially when the demand of precision and stability is more high with the development of high speed and precision rotating machinery. Ahmed et al. [1] presented a study of the effect of misalignment on the dynamic characteristics of journal bearings. Félix et al. [2] analyzed the effect of surface roughness in hydrodynamic bearings using the finite differences discretization techniques and multigrid methods. Wang et al. [3, 4] computed the characteristics of journal bearings lubricated with micropolar fluids considering cavitating effects. Shinde et al. [5] investigated the performance characteristics of conical shape hydrodynamic journal bearing with partial texturing, and results showed that bearing surface with partial texturing along 900–1800 region resulted in 42.08 % enhancement in maximum fluid film pressure compared with smooth surface.

In recent years, many researchers studied the effect of structural parameters on the characteristics of different structural bearings. Ahmada et al. [6] studied experimentally the effect of oil groove location on the temperature and pressure of hydrodynamic journal bearing. Xie et al. [7] specified the effect of journal rotation speed on pressure, load, components of oil film, and stress of bearing. Dwivedi et al. [8] studied the effect of recess length and width variation, number of recess variation on the load bearing capacity, and oil flow parameter for four-pocket rectangular recess hybrid journal bearing. Li et al. [9] found that carrying capacity of water lubricated bearings increased with the increase of grooves' size. Liang et al. [10, 11] calculated the recess pressure and flow of four-pocket capillary compensated hydrostatic bearing under different eccentricity ratios and wrap angles of oil recess. Shinde et al. [12] pointed out that bearing surface with partial groove along 90°–180° region can improve load capacity 75.9 percent compared with common journal bearing. Jiang et al. [13] studied the characteristics of thrust bearing for three types of inlet ramps and four different depths of linear ramp. Rashidi et al. [14] studied the tilt angle effects on the linear dynamic

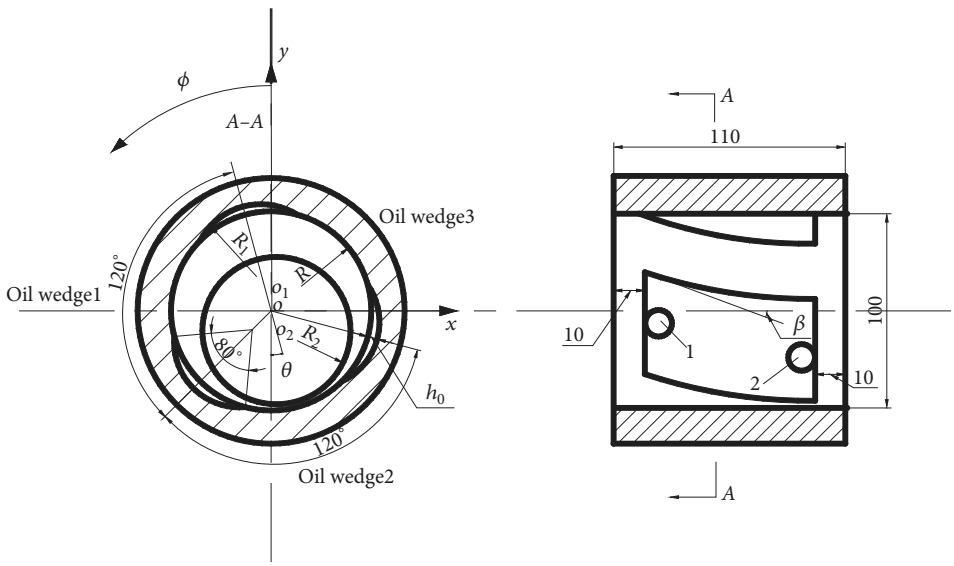

Figure 1: The structural diagram of spiral oil wedge sleeve bearing.

analysis of micropolar lubricated circular and multiple lobe journal bearings. Qin et al. [15] investigated the influences of oil groove parameters on the performance of journal bearing. Brito et al. [16] analyzed the effect of grooves in single and twin axial groove journal bearings under variable loading directions using a thermohydrodynamic approach. Guo [17] studied the influence of the shape, location, and geometric parameters of the dimples on the load capacity of journal bearing at different eccentricities. Spiral oil wedge sleeve bearing (see Figure 1) is a special structure sleeve bearing, which has three titled spiral oil wedges in circumferential direction. Chen et al. [18] studied the influence of outlet hole on the performance of spiral oil wedge hybrid journal bearing. Wang et al. [19] studied the influence of critical shear stress on wall slip of spiral oil wedge journal bearing. Spiral angel is an important structure parameter of spiral oil wedge sleeve bearing, which produces greater impact on bearing performance. The spiral angle study of spiral oil wedge journal bearing is rare, and influence of spiral angle on the static and dynamic characteristics of spiral oil wedge sleeve bearing is studied by numerical calculation.

2. Theoretical Model

2.1. The Equation of Spiral Angle. As shown in Figure 1, spiral oil groove bearing has three oil grooves and has oil return hole 1 and oil feed hole 2 at two ends of every oil groove, and its surface has two parts: the common surface and circular recess surface formed by three oil grooves; oil film thickness is calculated as follows.

The oil film thickness of common surface can be expressed as

$$h = c + e\cos(\phi - \theta). \tag{1}$$

The oil film thickness of circular recess surface is as follows:

$$h = c + e\cos(\phi - \theta) + R_1\cos\gamma + e_1\cos(\phi - \alpha) - R$$
$$\cos\gamma = \sqrt{1 - \left[\frac{e_1\sin(\phi - \alpha)}{R_1}\right]^2}, \tag{2}$$

where α denotes the position angle of the eccentric arc, $\alpha = ztg\beta/R$, β is spiral angle, h is oil film thickness, e is eccentricity, c is bearing radial clearance, θ is attitude angle, R is bearing radius, R_1 denotes the radius of the arc surface, e_1 denotes the eccentricity of the eccentric arc, and ϕ is angular coordinate.

2.2. The Generalize Reynolds Equation with Wall Slip and JFO Boundary Condition. In the condition of high speed and super high speed, the shear stress of solid-liquid interface can exceed critical shear stress, and wall slip occurs. The traditional Reynolds boundary condition is fit for oil film rupture boundary but cannot explain the oil film reformation condition correctly; Jakobsson-Floberg-Olsson (JFO) boundary condition can ensure the mass conservation of oil film rupture location and reformation position. Therefore the generalize Reynolds equation considering wall slip is gained based on JFO boundary condition, which will be benefit for knowing lubrication characteristics of high speed journal bearing.

Critical shear stress model thinks that wall slip occurs when shear stress is larger than critical shear stress, then the value of shear stress is critical shear stress. The surface circle of spiral oil wedge sleeve bearing is not continuous, the working clearance of bearing is circumferential and axial function, so the circumferential and axial wall slip is considered when the

numerical model is set; the models of four conditions are set separately. The four slip states are as follows: wall slip can not occur on the axial surface and sleeve surface, wall slip can only occur on the sleeve surface, wall slip can only occur on the axial surface, and wall slip can occur on the axial surface and sleeve surface [19].

When wall slip occurs on the axial surface and sleeve surface, the resultant shear stress is larger than critical shear stresses τ_{cul} and τ_{cdl}, then shear stress τ_{yx} in x direction is equal to $\tau_{\text{cul}x}$ and $\tau_{\text{cdl}x}$, and shear stress τ_{yz} in z direction is equal to $\tau_{\text{cul}z}$ and $\tau_{\text{cdl}z}$.

$$\begin{aligned}
&\tau_{yx} = \beta_{\text{cul}x}\tau_{\text{cul}x},\\
&\tau_{yz} = \beta_{\text{cul}z}\tau_{\text{cul}z}\\
&\qquad\qquad \text{At } y = h,\ \sqrt{\tau_{yx}^2 + \tau_{yz}^2} > \tau_{\text{cul}}\\
&\tau_{yx} = \beta_{\text{cdl}x}\tau_{\text{cdl}x},\\
&\tau_{yz} = \beta_{\text{cdl}z}\tau_{\text{cdl}z}\\
&\qquad\qquad \text{At } y = 0,\ \sqrt{\tau_{yx}^2 + \tau_{yz}^2} > \tau_{\text{cdl}},
\end{aligned} \tag{3}$$

where τ_{yx} is the shear stress in the x direction, x is circumferential coordinates, τ_{yz} is the shear stress in the z direction, z is axial coordinates, $\beta_{\text{cul}x}$, $\beta_{\text{cul}z}$, $\beta_{\text{cul}x}$, and $\beta_{\text{cul}z}$ are sign functions, $\tau_{\text{cul}x}$ is the critical shear stress of sleeve surface in x direction, $\tau_{\text{cul}z}$ is the critical shear stress of sleeve surface in z direction, y is radial coordinates, h is oil film thickness, τ_{cul} and τ_{cdl} are critical shear stress for slip at sleeve and axial surface, and $\tau_{\text{cul}} = \sqrt{\tau_{\text{cul}x}^2 + \tau_{\text{cul}z}^2}$.

Using boundary condition (3) and substituting the simplified N-S equation, the generalized Reynolds equation considering the wall slip of axial surface and sleeve surface is as follows:

$$\begin{aligned}
&\frac{\partial}{\partial x}\left(h^3\frac{\partial p}{\partial x}\right) + \frac{\partial}{\partial z}\left(h^3\frac{\partial p}{\partial z}\right)\\
&\quad = 2\left(\beta_{\text{cul}x}\tau_{\text{cul}x} - \beta_{\text{cdl}x}\tau_{\text{cdl}x}\right)h\frac{\partial h}{\partial x}\\
&\qquad + 2\left(\beta_{\text{cul}z}\tau_{\text{cul}z} - \beta_{\text{cdl}z}\tau_{\text{cdl}z}\right)h\frac{\partial h}{\partial z},
\end{aligned} \tag{4}$$

where p is oil film pressure.

Similarly, the generalized Reynolds equations of remaining three slip states are obtained.

Based on JFO boundary condition, switch function modifies Reynolds equation which is similar with the application of Elrod method. Elrod method regards that the lubrication is compressible fluid, gets the relation of density and pressure, and controls that the full oil film region is 1 and cavitation region is 0 by switch function g [3, 4].

$$p = p_{\text{cav}} + g\beta_t \ln\left(\alpha_\rho\right). \tag{5}$$

$\ln(\alpha_\rho)$ can be simplified by Taylor series as follows:

$$p = p_{\text{cav}} + g\beta_t\left(\alpha_\rho - 1\right), \tag{6}$$

where p_{cav} is the pressure of cavitation region, β_t is the lubricant bulk modulus, and α_ρ is the nondimensional density.

Elrod used the change of density to reflect the continuous of oil film in cavitation region in the generalized Reynolds equation. Substituting $p_p = \beta_t(\alpha_\rho - 1)$ and (6) into (4) considering the change of density,

$$\begin{aligned}
&\frac{\partial}{\partial\phi}\left(\overline{H}^3 g\frac{\partial\overline{p}_\rho}{\partial\phi}\right) + \left(\frac{1}{2Xi}\right)^2\frac{\partial}{\partial\lambda}\left(\overline{H}^3 g\frac{\partial\overline{p}_\rho}{\partial\lambda}\right)\\
&\quad = \frac{\beta_{\text{cul}x}T_{\text{cul}x}\overline{H}}{3\overline{\beta}_t}\frac{\partial\left(\overline{p}_\rho\overline{H}\right)}{\partial\phi} + \frac{\beta_{\text{cul}x}T_{\text{cul}x}\overline{H}}{3}\frac{\partial\overline{H}}{\partial\phi}\\
&\qquad + \frac{\beta_{\text{cul}z}RT_{\text{cul}z}\overline{H}}{3L\overline{\beta}_t}\frac{\partial\left(\overline{p}_\rho\overline{H}\right)}{\partial\lambda} + \frac{\beta_{\text{cul}z}RT_{\text{cul}z}\overline{H}}{3L}\frac{\partial\overline{H}}{\partial\lambda}\\
&\qquad - \frac{\beta_{\text{cdl}x}T_{\text{cdl}x}\overline{H}}{3\overline{\beta}_t}\frac{\partial\left(\overline{p}_\rho\overline{H}\right)}{\partial\phi} - \frac{\beta_{\text{cdl}x}T_{\text{cdl}x}\overline{H}}{3}\frac{\partial\overline{H}}{\partial\phi}\\
&\qquad - \frac{\beta_{\text{cdl}z}RT_{\text{cdl}z}\overline{H}}{3L\overline{\beta}_t}\frac{\partial\left(\overline{p}_\rho\overline{H}\right)}{\partial\lambda} - \frac{\beta_{\text{cdl}z}RT_{\text{cdl}z}\overline{H}}{3L}\frac{\partial\overline{H}}{\partial\lambda}\\
&\qquad + \frac{2}{\overline{\beta}_t}\frac{\partial\left(\overline{p}_\rho\overline{H}\right)}{\partial t} + 2\frac{\partial\overline{H}}{\partial t}.
\end{aligned} \tag{7}$$

Similarly, the generalized Reynolds equations of remaining three conditions based on JFO boundary condition are obtained.

3. Numerical Calculation

The generalized Reynolds equations of four slip conditions based on JFO boundary condition are solved using finite difference method. Perturbation pressure Reynolds equations are solved using the concept of partial derivatives and stiffness and damping coefficients of sleeve bearing are calculated [20]. The primary parameters of the studied bearing are shown in Table 1.

4. Numerical Results and Analysis

4.1. Static Characteristics of Bearing at Different Spiral Angles. Figures 2 and 3 are the effect of spiral angle β on dimensionless carrying capacity and friction drag. The figures show that the carrying capacity and friction drag of oil film decrease, and the decrease trend becomes smoother with the increase of spiral angle. The reason is as follows: the flow velocity of lubrication oil along axial direction increases, the lubrication oil flows out of bearing by end leakage and outlet hole, the dynamic effect weakens, and carrying capacity decreases with the increase of spiral angle. The carrying capacity and friction drag are smaller considering wall slip and JFO condition compared with reckoning with no slip and Reynolds boundary condition. For example, in the case of $\beta = 0.2$ and $\beta = 0.8$, carrying capacity is about 72.7% and

Table 1: Primary parameters of spiral oil wedge sleeve bearing.

parameter	symbol	unit	value
Bearing width	L	mm	110
Bearing radius	R	mm	50
Bearing radial clearance	c	mm	0.02
Depth of the arc groove	h_0	mm	0.12
Rotational speed	N	r/min	10000
Inlet oil pressure	P_{in}	MPa	0.3
Cavitation pressure	p_{cav}	MPa	−0.072
Oil viscosity	η	Pa·s	0.0018

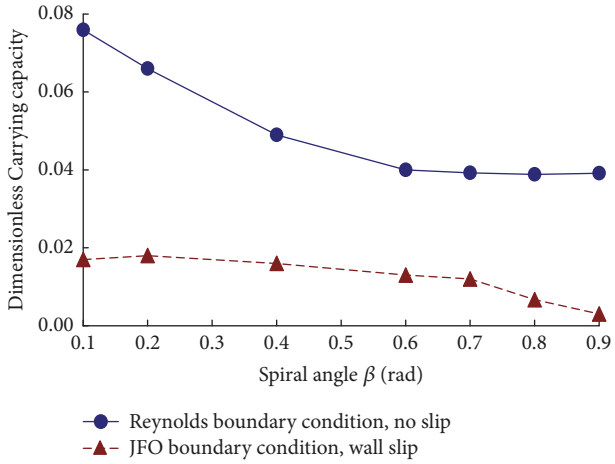

Figure 2: Carrying capacity.

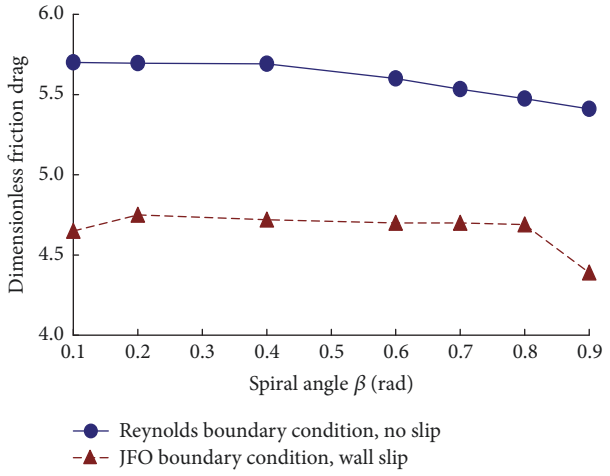

Figure 3: Friction drag.

82.8% smaller considering wall slip and JFO condition than reckoning with no slip and Reynolds boundary condition; friction drag is about 16.6% and 14.3% smaller considering wall slip and JFO condition than reckoning with no slip and Reynolds boundary condition. The decrease of friction drag is benefit for improving the characteristics of bearing, and the decrease of carrying capacity is no benefit, so the wall slip should be used reasonably to realize the drag reduction of bearing surface.

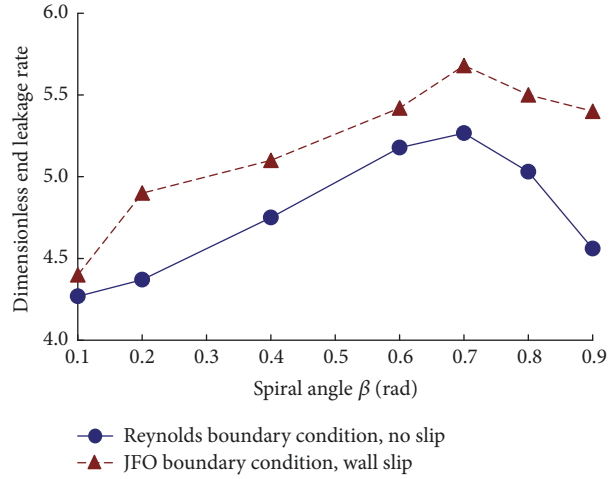

Figure 4: End leakage rate.

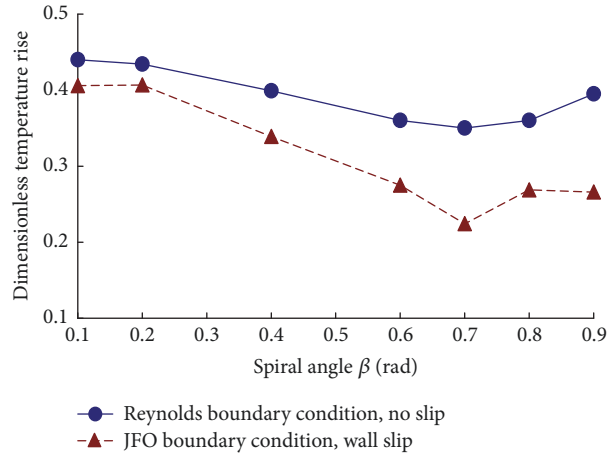

Figure 5: Temperature rise.

Figures 4 and 5 are the effect of spiral angle β on dimensionless end leakage rate and temperature rise. The figures show that, with the increase of spiral angle, the end leakage rate increases and temperature rise decreases at $\beta < 0.7$, end leakage rate decreases, and temperature rise increases at $\beta > 0.7$. This is mainly because the lubrication oil flows out of bearing more by end leakage and outlet hole, the end leakage increases, and temperature rise decreases with the increase of spiral angle. The end leakage rate is higher and temperature rise is smaller considering wall slip and JFO condition compared with reckoning with no slip and Reynolds boundary condition. For example, in the case of $\beta = 0.2$ and $\beta = 0.8$, end leakage is about 12.1% and 9.3% higher considering wall slip and JFO condition than reckoning with no slip and Reynolds boundary condition, and temperature rise is about 6.3% and 15% lower considering wall slip and JFO condition than reckoning with no slip and Reynolds boundary condition. The increase of end leakage and the decrease of temperature rise are benefit for improving the rotating speed of high speed bearing, but spiral angle is not better at bigger value, and there is an optimal value of 0.7.

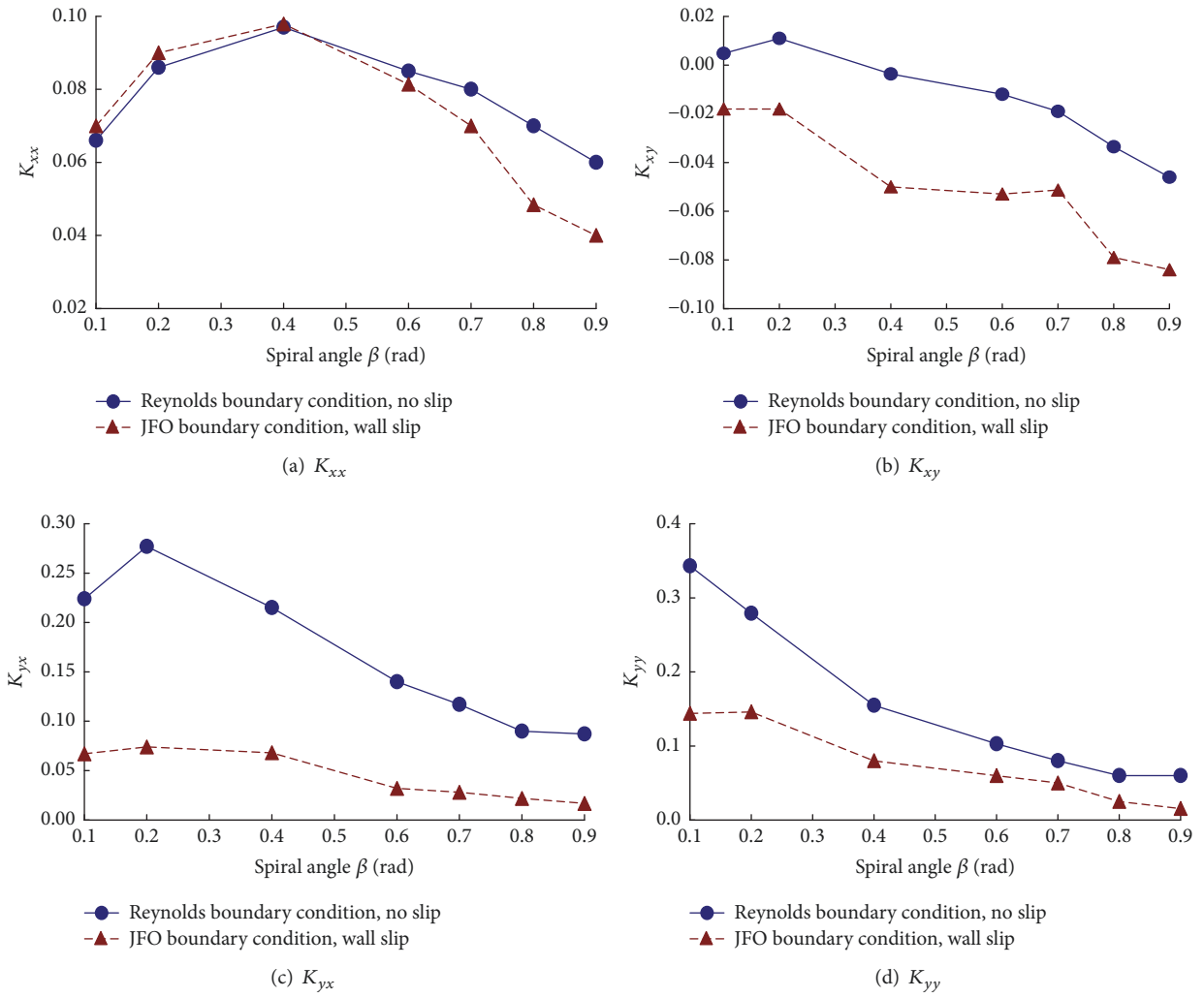

Figure 6: Stiffness coefficients.

4.2. Dynamic Characteristics of Bearing at Different Spiral Angles. The dynamic characteristics of bearing reflect the change of the oil film force when the journal deviates from the static equilibrium position and performs the displacement movement near this position, which has a greater impact on the performance of the entire bearing rotor system. Under the assumption of small amplitude, the instantaneous displacement and the instantaneous speed based on the journal center deviating from the static equilibrium position can be defined as the stiffness coefficients and the damping coefficients of bearing. Figure 6 is the effect of spiral angle β on stiffness coefficients K_{xx}, K_{xy}, K_{yx}, and K_{yy}. The figures show that, with the increase of spiral angle, stiffness coefficients K_{xx}, K_{xy}, and K_{yx} increase first and then decrease, and K_{yy} decreases, which proves that stiffness coefficient is not better at bigger value and there is an optimal value. The stiffness coefficients are lower generally considering wall slip and JFO condition compared with reckoning with no slip and Reynolds boundary condition. As the preceding analysis of static characteristics, the carrying capacity is smaller considering wall slip and JFO condition compared with reckoning with no slip and Reynolds boundary condition; the ability of resistance for disturbance decreases.

Figure 7 is the effect of spiral angle β on damping coefficients B_{xx}, B_{xy}, B_{yx}, and B_{yy}. The figures show that, with the increase of spiral angle, damping coefficients B_{xx}, B_{xy}, B_{yx}, and B_{yy} increase first and then decrease, which proves that damping coefficient is not better at bigger value and there is an optimal value. The damping coefficients are lower generally considering wall slip and JFO condition compared with reckoning with no slip and Reynolds boundary condition, and the decrease is not obvious at bigger spiral angle. For example, in the case of $\beta = 0.7$, damping coefficients B_{xx}, $B_{xy}(B_{yx})$, and B_{yy} are about 0.0023, 0.045, and 0.038 lower considering wall slip and JFO condition than reckoning with no slip and Reynolds boundary condition.

5. Conclusions

The conclusions can be summarized as follows.

(1) With the increase of spiral angle, carrying capacity and friction drag of oil film decrease, the end leakage rate

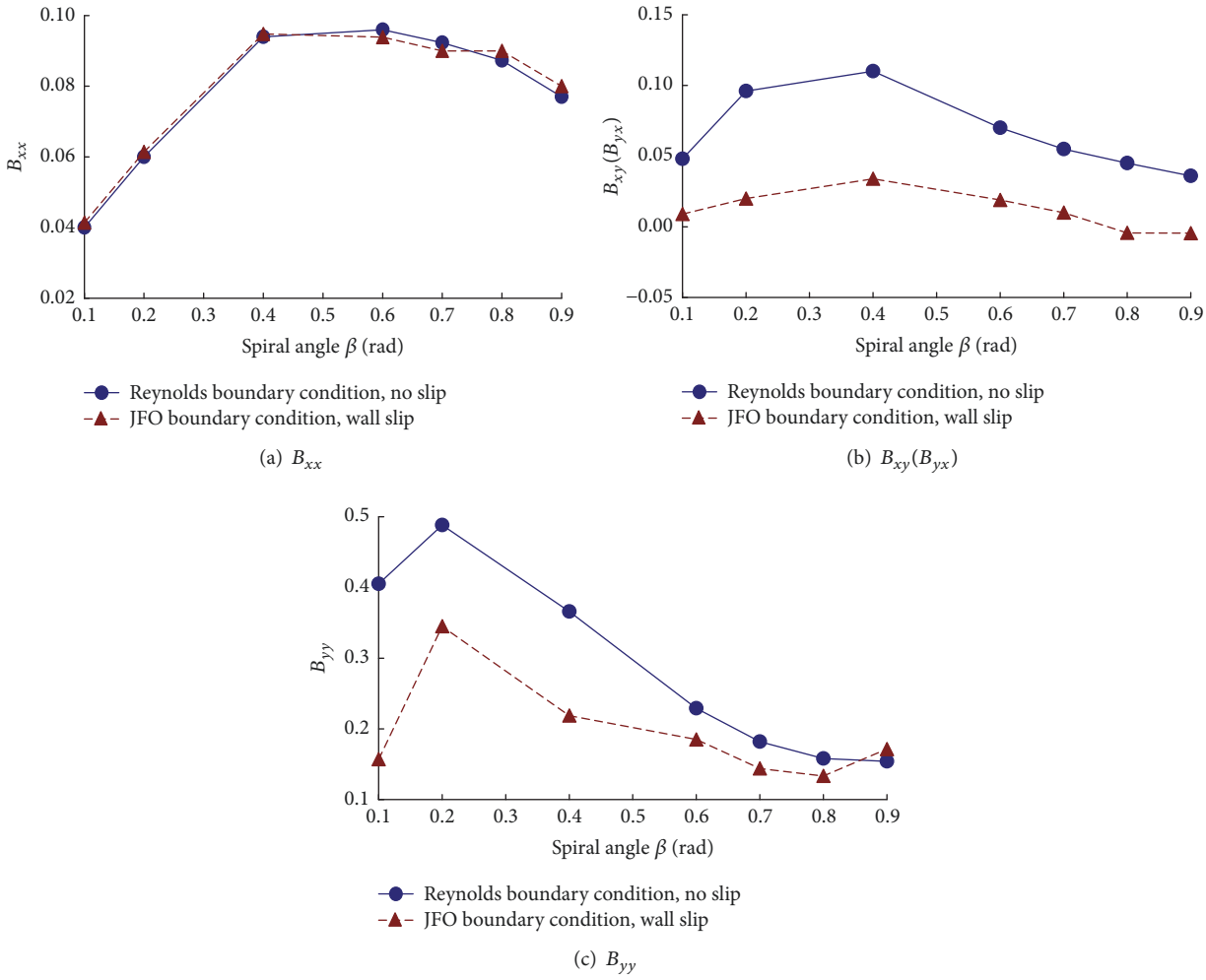

Figure 7: Damping coefficients.

increases first and then decreases, and temperature rise decreases first and then increases; when spiral angle is 0.7, the temperature rise is minimal and end leakage rate is maximum, and the optimal value of spiral angle for the two properties is 0.7.

(2) The carrying capacity, friction drag, and temperature rise are smaller and the end leakage rate is higher considering wall slip and JFO condition compared with reckoning with no slip and Reynolds boundary condition. The decrease of friction drag and temperature rises, and the increase of end leakage is benefit for improving the characteristics of high bearing; the decrease of carrying capacity is no benefit. So when the wall slip is used for improving the characteristics of bearing, the wall slip region of higher shear stress for combined slip surface bearing should be optimized.

(3) With the increase of spiral angle, stiffness coefficients and damping coefficients generally increase first and then decrease. The stiffness coefficient and damping coefficients are lower generally considering wall slip and JFO condition compared with reckoning with no slip and Reynolds boundary condition. Spiral angle has different effect on dynamic coefficients; K_{xx}, B_{xx}, B_{xy}, and B_{yx} are best when spiral angle is 0.4, but almost other dynamic coefficients are best when spiral angle is 0.2; the optimum spiral angle should be determined by optimizing the design in order to make bearing have better dynamic characteristics and vibration resistance.

Conflicts of Interest

The authors declare that they have no conflicts of interest.

Acknowledgments

This work was supported by the grant from China Postdoctoral Science Foundation Funded Project (no. 2017M612304), Shandong Provincial Postdoctoral Innovation Foundation (no. 201701016), SDUST Research Fund (no. 2015JQJH104), and Qingdao Postdoctoral Research Funded Project and National Natural Science Foundation of China (no. 51305242).

References

[1] A. M. Ahmed and A. El-Shafei, "Effect of misalignment on the characteristics of journal bearings," *Journal of Engineering for Gas Turbines and Power*, vol. 130, no. 4, Article ID 042501, 2008.

[2] A. Félix Quiñonez and G. E. Morales-Espejel, "Surface roughness effects in hydrodynamic bearings," *Tribology International*, vol. 98, pp. 212–219, 2016.

[3] X.-L. Wang and K.-Q. Zhu, "Numerical analysis of journal bearings lubricated with micropolar fluids including thermal and cavitating effects," *Tribology International*, vol. 39, no. 3, pp. 227–237, 2006.

[4] X.-L. Wang, J.-Y. Zhang, and H. Dong, "Analysis of bearing lubrication under dynamic loading considering micropolar and cavitating effects," *Tribology International*, vol. 44, no. 9, pp. 1071–1075, 2011.

[5] A. Shinde, P. Pawar, P. Shaikh, S. Wangikar, S. Salunkhe, and V. Dhamgaye, "Experimental and Numerical Analysis of Conical Shape Hydrodynamic Journal Bearing With Partial Texturing," *Procedia Manufacturing*, vol. 20, pp. 300–310, 2018.

[6] M. A. Ahmad, S. Kasolang, and R. S. Dwyer-Joyce, "Experimental study on the effects of oil groove location on temperature and pressure profiles in journal bearing lubrication," *Tribology International*, vol. 74, pp. 79–86, 2014.

[7] Y. Xie, B. Zhang, and Y. M. Hu, "Effect of journal rotation speed on characteristic of oil film and structural characteristic of bearings," *Lubrication engineering*, vol. 40, no. 11, pp. 23–29, 2005.

[8] V. K. Dwivedi, S. Chand, and K. N. Pandey, "Effect of number and size of recess on the performance of hybrid (hydrostatic/hydrodynamic) journal bearing," in *Proceedings of the 3rd Nirma University International Conference on Engineering, NUiCONE 2012*, pp. 810–817, ind, December 2012.

[9] Li. ZY, D. Jiang, and Z. W. Yin, "Effect analysis of grooves on water film pressure distribution of water-lubricated bearings," *Journal of Donghua University*, vol. 38, no. 5, pp. 509–513, 2012.

[10] P. Liang, C. Lu, W. Pan, and S. Li, "A new method for calculating the static performance of hydrostatic journal bearing," *Tribology International*, vol. 77, pp. 72–77, 2014.

[11] P. Liang, C. Lu, and F. Yang, "Study on static performance of a new type of standard elliptical four-pocket hybrid journal bearing," *Journal of the Balkan Tribological Association*, vol. 21, no. 4, pp. 1010–1016, 2015.

[12] B. Shinde Anil and M. Pawar Prashant, "Effect of partial grooving on the performance of hydrodynamic journal bearing.Industrial Lubrication," *Journal of Tribology*, vol. 69, no. 4, pp. 574–584, 2017.

[13] X. L. Jiang, J. H. Fang, and J. G. Wang, "Effects of inlet ramps on thermohydrodynamic lubrication of thrust bearing," *Lubrication Engineering*, vol. 35, no. 6, pp. 24–28, 2010.

[14] R. R. Meybodi, M. Z. Mehrjardi, and A. D. Rahmatabadi, "Tilt angle effects on the performance of micropolar lubricated non-circular journal bearings," *Industrial Lubrication and Tribology*, vol. 69, no. 4, pp. 536–549, 2017.

[15] Y. Qin, Z. M. Zhang, Q. Zhou, and Q. An, "Influences of oil groove parameters on performance of journal bearing," *Journal of East China University of Science and Technology*, vol. 36, no. 5, pp. 125–131, 2010.

[16] F. P. Brito, A. S. Miranda, and M. Fillon, "Analysis of the effect of grooves in single and twin axial groove journal bearings under varying load direction," *Tribology International*, vol. 103, pp. 609–619, 2016.

[17] B. Guo, "Optimal surface texture design of journal bearing with axial grooves," *International Journal of Heat and Technology*, vol. 35, no. 2, pp. 267–272, 2017.

[18] S. J. Chen, L. u. CH, and J. K. Ma, "Influence of the outlet hole on performance of a spiral oil wedge hybrid journal bearing," *Lubrication Engineering*, vol. 32, no. 9, pp. 12–15, 2007.

[19] L.-L. Wang, C.-H. Lu, P.-Q. Ge, and S.-J. Chen, "Study on the influence of critical shear stress on wall slip of spiral oil wedge journal bearing," *Proceedings of the Institution of Mechanical Engineers, Part J: Journal of Engineering Tribology*, vol. 226, no. 5, pp. 362–376, 2012.

[20] Z. M. Zhang, *Hydrodynamic lubrication theory of sliding bearing*, Higher Education Press, 1986.